

MVAC XLPE Cables for MVDC – DC Conductivity of Plaque Samples During Temperature Changes

Patrik Ratheiser¹, Uwe Schichler^{1,2}

¹*Institute of High Voltage Engineering and System Performance, Graz University of Technology*

²*High Voltage Test Laboratory Graz Ltd.*

Graz, Austria

patrik.ratheiser@tugraz.at

Abstract

The rising demand for electric energy poses increasing challenges for the distribution grid. To overcome these challenges, direct current (DC) transmission will play a dominant role in the medium voltage (MV) level. On the one hand, MV alternating current (AC) cable systems can be converted into MVDC cable systems and, on the other hand, new MVDC cable systems can be implemented into the existing grid.

However, MVDC cables with extruded insulation show special phenomena (e.g. space charges). Due to the interest in characteristics of this insulation this paper provides information about the DC conductivity of XLPE plaque samples during steady thermal and electric stress and during temperature changes. The plaque samples are extracted from 12/20 kV MVAC XLPE cables. The DC conductivities at steady state and during temperature changes are presented in a temperature range from 25 °C – 90 °C and an electrical stress up to 30 kV/mm.

1. Introduction

In the context of the energy transition, the transportation and distribution of climate-friendly energies presents major challenges. A solution is DC transmission in the high voltage (HV) and in the MV level. Currently, HVDC transmission shows major growth. The project NEMO-Link is the first ± 400 kV DC XLPE submarine cable link to connect the United Kingdom and Belgium [1]. Furthermore, ± 525 kV DC XLPE cables are being developed and used in projects in Germany [2].

Due to the growing energy production, the importance of MVDC transmission systems will increase significantly in the future. MVDC transmission offers advantages such as the high transmission capacity. Great interest exists in converting the existing MVAC cable systems to MVDC and in installing new MVDC cable systems [3 – 7].

In the project Angle-DC in Wales, a 33 kV AC line consisting mainly of cables is being converted into a ± 27 kV MVDC system [8]. Furthermore, a 12/20 kV AC XLPE cable system, including the corresponding AC accessories, has been tested successfully in a line-commutated converter (LCC) prequalification test and an LCC type test for a nominal DC voltage of $U_{DC} = \pm 55$ kV in accordance with CIGRE TB 852 [3, 4, 9]. This resulted in an approach for a qualification procedure for MVAC cable systems for DC operation [5]. The previously mentioned qualification procedure involves additional tests

and simulations. Furthermore, the testing of MVDC cable systems is discussed by CIGRE WG B1.82 “Medium Voltage DC Cable System Requirements”.

This paper describes the outcome of DC leakage current measurements performed on XLPE plaque samples. The DC conductivity is obtained from the leakage current of the MVDC cable insulation. The plaque samples are taken from standard 12/20 kV AC XLPE cables (Fig. 1). The apparent DC conductivity is presented within an applied electric stress range of 0.3 kV/mm – 20 kV/mm under steady state operation conditions and with temperatures ranging from 25 °C – 90 °C. Furthermore, measurements of DC conductivity were carried out during temperature changes and the application of constant electric stress ranging from 10 kV/mm – 30 kV/mm.

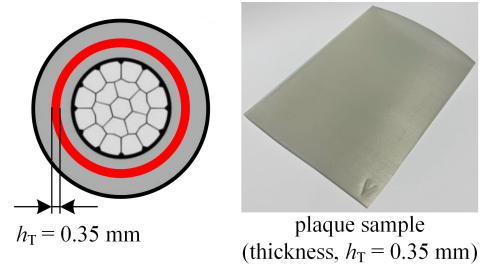


Fig. 1 - XLPE plaque sample taken from the insulation of a 12/20 kV MVAC XLPE cable

2. Theoretical background

2.1. DC leakage current and approximation of DC conductivity

By applying a voltage step, positive and negative charge carriers drift in the opposite direction due to the Coulomb force. The DC leakage current $i_{\text{leak}}(t)$ through insulation material can be explained as a superposition of four currents (Eq. 1). These currents display time-dependent behaviour and consist of the charging current $i_l(t)$, the polarization current $i_p(t)$, the current from the existing space charges $i_{sc}(t)$ and the conduction current $i_c(t)$ [10].

$$i_{\text{leak}}(t) = i_l(t) + i_p(t) + i_{sc}(t) + i_c(t) \quad (1)$$

When a voltage step is applied, polarization effects influence the DC leakage current. After a certain period of time, the current reaches a steady state. Due to the fact that the steady state can only theoretically be reached during measurements, the DC conductivity is referred to

as the apparent DC conductivity. When the voltage is switched off, depolarization currents occur which decrease to zero after a certain amount of time. The DC conductivity depends on the applied electric stress, temperature and time. It shows a strong nonlinear behaviour with respect to these parameters. The DC conductivity strongly influences the electric field in the insulation material. These influences must be taken into account by applying DC voltage to the equipment. Eqs. 2 – 4 show how the DC conductivity can be modelled based on the hopping conduction (Eq. 2), the Poole-Frenkel equation (Eq. 3) and an empirical equation (Eq. 4). The empirical equation can be used to obtain an accurate approximation in many applications.

$$\sigma(E, \vartheta) = \frac{A}{E} \cdot e^{\left(-\frac{B}{k_B \cdot \vartheta}\right)} \cdot \sinh\left(\frac{C}{\vartheta} \cdot E\right) \quad (2)$$

$$\sigma(E, \vartheta) = D \cdot e^{\left(-\frac{B}{k_B \cdot \vartheta}\right)} \cdot e^{\left(\frac{F}{\vartheta} \cdot \sqrt{E}\right)} \quad (3)$$

$$\sigma(E, \vartheta) = \sigma_0 \cdot e^{\alpha \cdot \vartheta} \cdot e^{\beta \cdot E} \quad (4)$$

where σ is the DC conductivity, E is the electric stress, ϑ is the temperature, k_B the Boltzmann constant, and A , B , C , D , F , α , β are constants. The physical basis of the equations is described in [11 – 13]. Each equation has its own scope. The scopes depend on the insulation material, the operating temperature and the used electric field strength. For example, the hopping conduction covers low levels of electric stress where the impact of the electric field on the activation energy is low. Eq. 3 and Eq. 4 are mostly used with insulation materials like XLPE. The electric field clearly has a higher impact on the DC conductivity in these equations [11, 13].

2.2. Space-charge-limited current conduction

The space charge accumulation is one parameter that can be recognised with DC leakage current measurements on plaque samples. Space charges accumulate in the insulation materials and manifest themselves in the DC leakage current curve as the “electric threshold” E_{TH} (Fig. 2). If space charges occur in the insulation, the behaviour of the DC conductivity changes strongly.

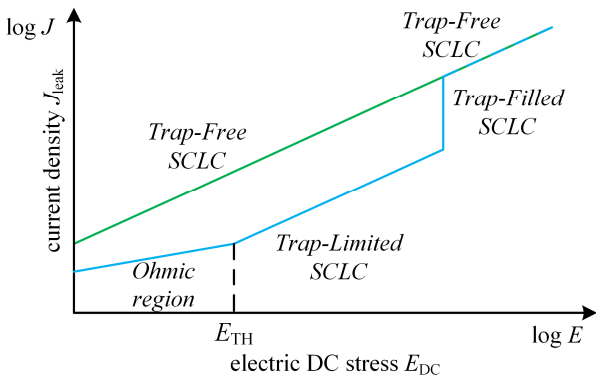


Fig. 2 - J - E characteristics in the presence of space-charge-limited current conduction [11]

The space-charge-limited current (SCLC) theory shows how the electric conductivity changes depending on the electric field. The accumulation of space charges results in a threshold after which the electric conductivity rises faster than in the ohmic region (trap-limited SCLC). If the electric stress increases still further, the current rises rapidly, and the traps in the material are completely filled with charges (trap-filled SCLC). After this, the trap-free SCLC is reached, and the current density rises in direct correlation with the applied electric stress [11].

3. Methodology

3.1. Test setup and test object

Fig. 3 shows the schematic laboratory setup including the test cell, which was used to measure the leakage current on XLPE plaque samples. It consisted of a HV electrode (diameter $d_o = 55$ mm), a ground electrode ($d_i = 43$ mm), a guard ring ($d_o = 55$ mm) to shield surface currents and a gap space ($g = 1$ mm). The measurement system was constructed in accordance with the IEC 62631-3-2 [14]. The leakage current through the test object was measured with a picoammeter (Keithley 6514), and a Keithley 705 scanner was used to measure plaque samples synchronized from various test cells.

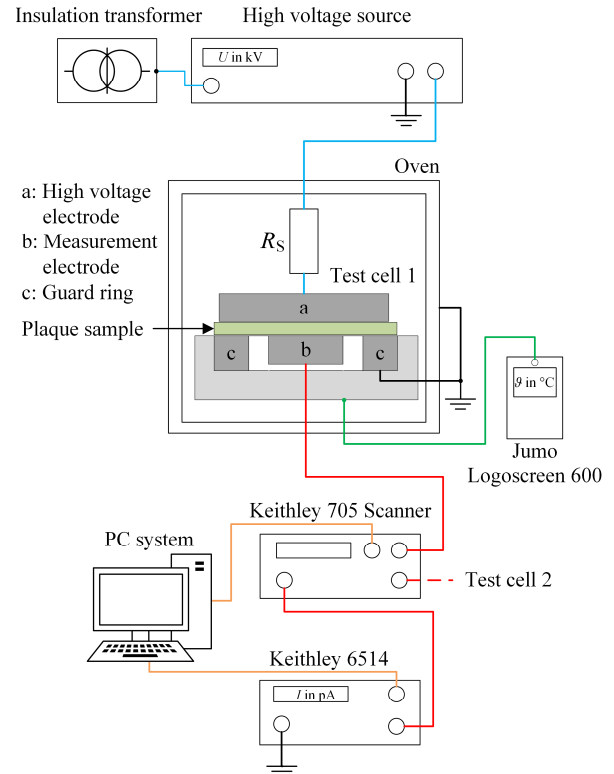


Fig. 3 - Schematic laboratory setup

The XLPE plaque samples have a thickness of approx. 0.35 mm and were taken from a new 12/20 kV MVAC XLPE cable. To measure the thickness of the XLPE plaque samples, a micrometre with a tolerance of ± 0.01 mm was used. To ensure equal conditions for all plaque samples, the plaque samples were preconditioned

in an oven for at least 24 h at a temperature of 70 °C. This process ensured that the plaque samples were not affected by contamination (e.g. humidity).

The leakage current was used to calculate the electric conductivity of the insulation. The DC conductivity was calculated from the leakage current I_{leak} , plaque sample thickness h_T , effective electrode surface A_{eff} and applied DC voltage U_{DC} (Eq. 5, 6).

$$\sigma = \frac{I_{\text{leak}} \cdot h_T}{A_{\text{eff}} \cdot U_{\text{DC}}} \quad (5)$$

$$A_{\text{eff}} = \pi \cdot \left(r_1 + B_c \cdot \frac{g}{2} \right)^2 \approx 1470 \text{ mm}^2 \quad (6)$$

3.2. Measurement procedures

Table 1 shows the measurements presented in this contribution. Two measurement procedures were followed to obtain the apparent DC conductivity and to determine the behaviour of the DC conductivity. The apparent conductivity was first determined by taking measurements under conditions of constant electric stress E and temperature ϑ (step test). In this case, the electric stress was applied to the plaque sample for a minimum duration of 2 h. When the measured leakage current reached an apparent steady state for at least 1 h, the high voltage supply was switched off, and depolarization was performed for at least 15 min. Following this, the voltage was set to the next voltage level. The measurements were done for 25 °C – 90 °C and up to an electric field stress of 20 kV/mm.

Table 1 - Test parameters for the leakage current measurements

Step Test	
Electric field E	0.3 kV/mm – 20 kV/mm
Conductor temperature ϑ	25 °C – 90 °C
Temperature Changes	
Electric field E	10 kV/mm – 30 kV/mm
Conductor temperature ϑ	25 °C – 75 °C

Furthermore, the DC conductivity was measured during constant electric stress and temperature changes. The temperature changes simulate the thermal behaviour of MVDC cables, hence the determined DC conductivity shows a practical performance during these measurements. The temperature profile is shown in Fig. 4.

The temperature profile starts with a conditioning phase at 50 °C. Afterwards, the temperature was reduced to 25 °C, which represents zero-load conditions. The temperature was subsequently increased to 50 °C and then to 75 °C. These temperature steps simulate the cable behaviour under load conditions. Next, the temperature was reduced to the initial 50 °C level. At each temperature step the plaque sample was at a constant temperature for at least 1 h. While the measurements were performed, the temperature was measured with a Jumo Logoscreen 600 on the ground electrode of the test cell. In preliminary tests, the temperature levels were

measured on the plaque samples. Each plaque sample was subjected to the temperature profile five times (total 120 h). The test was carried out on five plaque samples to ensure that the test results were reproducible.

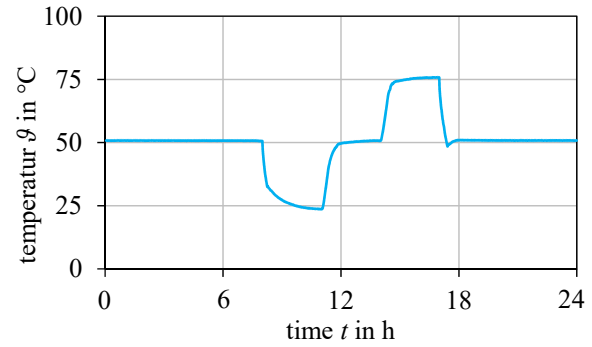


Fig. 4 - Temperature profile of the DC leakage current measurements

4. Results – electric conductivity during constant thermal and electric stress

4.1. Step test measurements during constant thermal and electric stress

The apparent DC conductivity (Eq. 5) is an important parameter of the insulation for the operation of cables under DC stress. The DC conductivity provides information about space charge accumulation in the insulation material. To recognise the space charge accumulation, leakage current measurements were done. The measurements were performed for a duration of at least 2 h for each temperature and electric field.

Fig. 5 shows the apparent conductivity of the investigated XLPE. The results show that the electric conductivity of the insulation plaque samples depends strongly on temperature and electric stress. At low electric fields, the DC conductivity is in the ohmic region (Fig. 2). The slope of nearly zero indicates that no space charges are occurring. When space charges occur, an electric threshold E_{TH} can be recognised. At higher electric fields the trap-limited SCLC was reached.

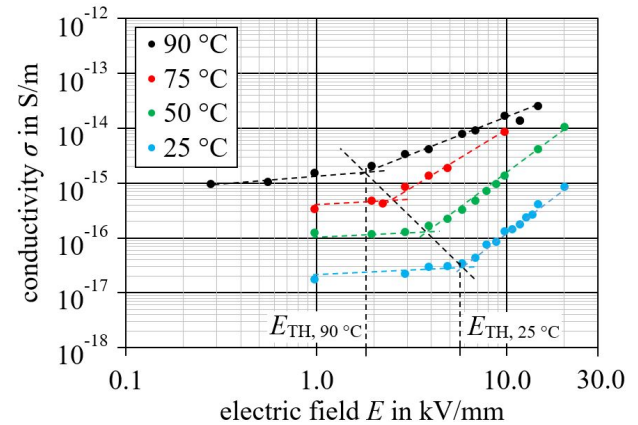


Fig. 5 - Results of the apparent conductivity measurements for constant electric stress and constant temperature

At room temperature (RT), the electric threshold occurred at approx. 6 kV/mm. At a temperature of 90 °C the electric threshold was observed at approx. 2 kV/mm. The results show that the thresholds for the different temperatures coincide on a line. The smaller electric threshold at higher temperature levels is related to the higher charge mobility. Moreover, the thermal energy is higher. Therefore, more charges can hop into the conduction band. The charges are also injected from the electrodes into the insulation material more easily at higher temperatures than at lower temperatures. The injected charges accumulate in the insulation bulk and increase the electric conductivity of the insulation [11].

4.2. Approximation of the apparent conductivity depending on electric stress and temperature

Fig. 6 shows the approximation of the apparent electric conductivity of the investigated XLPE. These results show that the electric conductivity increases as the electric stress and temperature increase. The conductivity is influenced more strongly by the applied temperature than by the electric stress. The obtained conductivity for an electric stress of $E = 10$ kV/mm ranges from 10^{-16} S/m (25 °C) to $2 \cdot 10^{-14}$ S/m (90 °C). The measurement data were fitted with the equations shown in chapter 2.1.

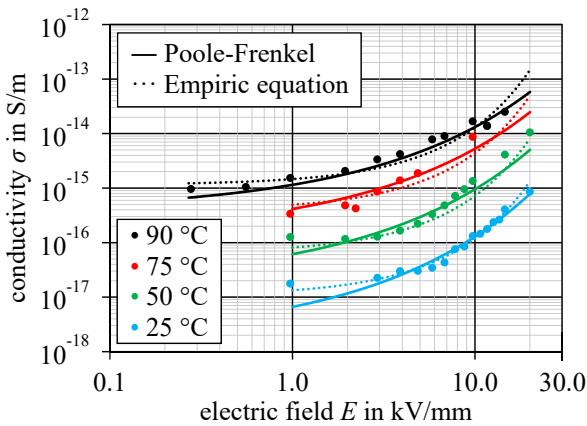


Fig. 6 - Approximation of the measurement results during constant temperature and electric field stress

The Poole-Frenkel equation and the empirical equation provide the best approximation for the measurements during constant thermal and electric stress with the smallest deviation of the logarithmic error function with $S = 5.8$ and $S = 6.4$, respectively. These are shown in Fig. 6. The approximation of the electric conductivity considering the Poole-Frenkel effect ($S = 5.8$) provides the best fit in this case. In comparison to the hopping conduction ($S = 11.2$), the Poole-Frenkel effect considers the energy impact of the electric field stress, which is necessary for space charges to escape a trap. Comparing the Poole-Frenkel effect with the empirical equation, it can be seen that both curves provide accurate results for the approximation of the electric conductivity. This may be due to the fact that the empirical equation was obtained from real measurement data in the past. Table 2 shows the parameters for the given equations.

Table 2 - Calculated parameters for the Poole-Frenkel effect, the hopping conduction and the empirical equation

Eq.	$A \left(\frac{S \cdot V}{m^2} \right)$	B (eV)	$C \left(K \cdot \frac{m}{V} \right)$	$D \left(\frac{S}{m} \right)$
(2)	147.2	0.747	$1.2 \cdot 10^{-4}$	
(3)		0.776		$21.5 \cdot 10^{-6}$
	$F \left(K \cdot \sqrt{\frac{m}{V}} \right)$	$\sigma_0 \left(\frac{S}{m} \right)$	$\alpha \left(\frac{1}{K} \right)$	$\beta \left(\frac{mm}{kV} \right)$
(3), (4)	0.410	$4.7 \cdot 10^{-27}$	0.072	0.243

5. Results – electric conductivity during temperature changes

To determine the electric conductivity of the insulation material for practical applications, the electric DC conductivity was measured during temperature changes. In real cable systems, the electric stress in the insulation is fixed, while the temperature changes due to the current. The temperature profile for this laboratory test is shown and described in chapter 3.2.

Fig. 7 shows the leakage current of an exemplary plaque sample. The plaque sample was placed under electric stress conditions of 10 kV/mm five times over a total of 120 h. The results show that the leakage current follows the temperature changes. Furthermore, the leakage current reduces as the number of cycles increases to reach a nearly steady state. The results show that the leakage current reduces from approx. 440 pA to 310 pA. This reduction may be related to the polarization of the insulation material and the accumulation of space charges in the insulation material over time.

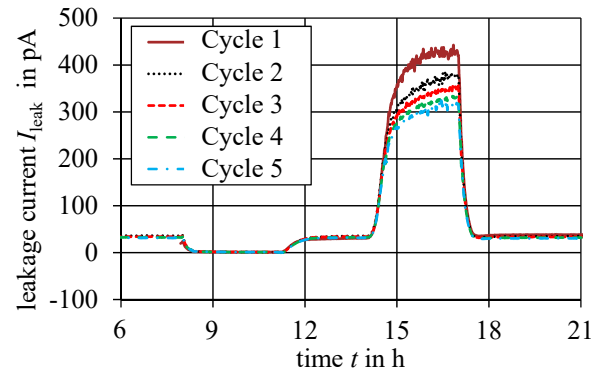


Fig. 7 - Leakage current of XLPE plaque sample over five cycles during temperature changes ($E = 10$ kV/mm)

Fig. 8 shows the electric conductivity of an exemplary plaque sample over five measurement cycles. The results show that the previously mentioned reduction in the leakage current does not lead to a significant change in the electric conductivity of the XLPE plaque samples (75 °C). This was observed for all measured plaque samples during temperature changes.

More closely examining the data, the leakage current was not observed to follow the temperature during the heating period from 25 °C to 50 °C in the first minutes of the test. Instead, a significant change was observed in the electric

conductivity as an undershoot (red ellipsis). This undershoot is visible at $E = 10$ kV/mm in 4 out of 5 plaque samples, while one plaque sample displayed an overshoot during the same increase in temperature. During the remaining changes in temperature, the change in the conductivity followed the temperature. No other significant effects were observed.

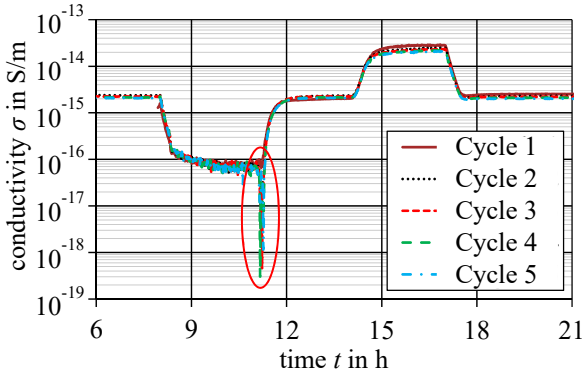


Fig. 8 - Electric conductivity of XLPE plaque samples over five measuring cycles during temperature changes (10 kV/mm)

Fig. 9 shows the significant decrease in the DC conductivity at an electric stress level of $E = 10$ kV/mm while the temperature changed from 25 °C to 50 °C. Because this decrease in the DC conductivity is not observed in the first cycle, the conditioning of the plaque sample seems to influence this phenomenon. Plaque samples were preconditioned for cycles two to five at 50 °C and an electric stress of $E = 10$ kV/mm. The significant decrease is observed for a period of 5 to 8 minutes and needs to be investigated in future.

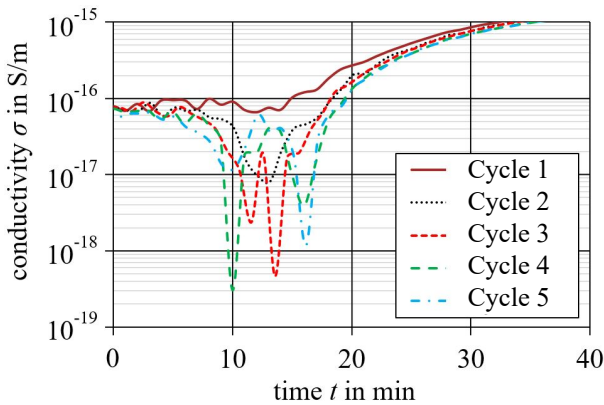


Fig. 9 - Unexpected significant decrease in the DC conductivity at an electric stress of $E = 10$ kV/mm

Fig. 10 shows an example of the DC conductivity within the range of 10 kV/mm – 30 kV/mm under changing temperature conditions in the third cycle. The unexpected significant decrease and increase (red ellipsis) occurred every time an electric stress of $E = 10$ kV/mm was applied. The unexpected significant decrease was observed 2 out of 5 times at an electric field stress of $E = 20$ kV/mm. It was not observed at an electric stress of $E = 30$ kV/mm. Therefore, this phenomenon seems to

depend on the applied electric stress. The undershoot or overshoot was also only visible within the temperature range of 25 °C – 50 °C, indicating that this phenomenon also depends on the applied temperature rise. The reason for this phenomenon needs to be investigated in further research. Furthermore, the results show that the specific conductivity of the investigated XLPE is less impacted by the electric stress with a rising electric stress.

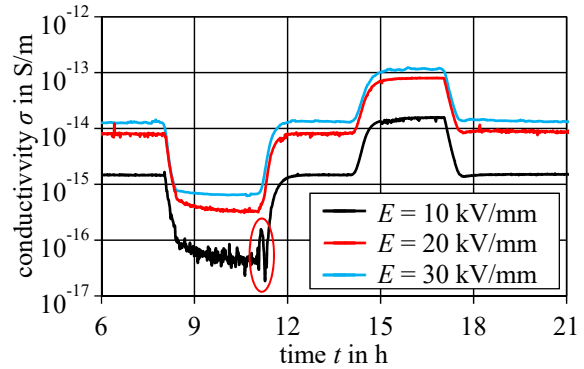


Fig. 10 - Electric conductivity on the third measuring cycle within the electric stress range of $E = 10$ kV/mm – 30 kV/mm

6. Comparison of results for the apparent conductivity at constant electric and thermal stress and during temperature changes

Fig. 11 shows the apparent conductivity in dependence of electric stress and temperature, which is visible in a range of 25 °C – 75 °C and 1 kV/mm – 30 kV/mm. The curves show the approximation of the measurement results during constant thermal and electric stress (Fig. 6). The triangles show the average of the data for the electric conductivity during temperature changes. These results show the scattering range of all measurements obtained under these conditions. These data were obtained during the last five minutes of every specific temperature step and electric stress. It can be seen, that the apparent conductivity during temperature changes correlates with the measurement data during constant thermal and electric stress.

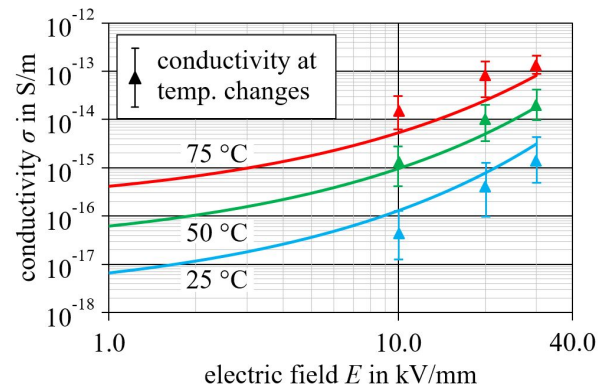


Fig. 11 - Comparison of the apparent conductivity under conditions of constant electric and thermal stress (Poole-Frenkel) and during temperature changes

The results clearly indicate that the apparent DC conductivity can be determined by taking leakage current measurements during temperature changes. These values should be compared to available data sets for the apparent conductivity of, e.g. XLPE to determine the range of electrical conductivity at different temperatures. With the apparent DC conductivity, the possibility of a thermal runaway and the presence of the field inversion in a cable system at the operating voltage level can be estimated and can be therefore recognised.

7. Discussion of the results

The apparent conductivity strongly depends on the electric field stress and temperature. An electric threshold and, therefore, an accumulation of space charges is indicated at 6 kV/mm for 25 °C and at 2 kV/mm for 90 °C. Three equations were used to approximate the apparent conductivity, and the results show that the Poole-Frenkel mechanism and the empirical equation are suitable for the investigated XLPE.

The measurements of the leakage current under conditions of constant electric stress during temperature changes show that the leakage current and the electric conductivity follow the material temperature. A significant change in the DC conductivity was noticeable when the temperature changed from 25 °C to 50 °C. For an increasing number of temperature cycles the leakage current reached a nearly steady state. This reduction in the leakage current had no significant impact on the DC conductivity. It is visible, that the DC conductivity shows nearly the same values for all measurements during temperature changes as under apparent steady state conditions. Therefore, temperature changes can be used to rapidly obtain data for the apparent conductivity of insulation materials in plaque samples.

8. Conclusion

The findings reported in this contribution demonstrate the impact of temperature changes on the DC conductivity of the insulation material XLPE. Normally, an MVDC cable is subjected to temperature changes during operation. To assess the impact of these temperature changes, the electric conductivity was compared to the apparent conductivity during constant thermal and electric stress. The measurements were carried out on XLPE plaque samples obtained from real 12/20 kV AC XLPE cables. The conductivity during constant thermal and electric stress in the temperature range of 25 °C – 90 °C shows that the electric threshold is temperature-dependent. Furthermore, the accumulation of space charges begins within the range of 2 kV/mm – 6 kV/mm.

The apparent electric conductivity during temperature changes follows the temperature with one peculiarity observed when the temperature changed from 25 °C to 50 °C. The DC conductivity after a temperature change shows nearly the same values as the apparent DC conductivity during constant electric and thermal stress.

Thus, the electric conductivity can be investigated during temperature changes with insulation plaque samples while changing the temperature and applying different voltage levels.

9. References

- [1] T. Igi et al., “Qualification, Installation and Commissioning of World’s First DC 400 kV XLPE Cable System”, Jicable’19, Versailles, France, 2019, Report A6-1.
- [2] A. Abbasi et al., “Performance Evaluation of 525 kV and 640 kV extruded DC Cable Systems”, Jicable’19, Versailles, France, 2019, Report A9-4.
- [3] P. Ratheiser, U. Schichler, “Review of IEC 62895 regarding Electrical Type Tests on extruded MVDC Cable Systems”, Jicable HVDC’21, Liège, Belgium, 2021.
- [4] A. Buchner, U. Schichler, “Review of CIGRE TB 496 regarding Prequalification Test on extruded MVDC Cables”, NORD-IS 19, Tampere, Finland, 2019, Report 26.
- [5] P. Ratheiser, U. Schichler, “Qualification of MVAC XLPE Cables for DC Operation”, ISH, Xi’an, China, 2021, Report 118.
- [6] P. Ratheiser, A. Buchner, U. Schichler, „Übertragungskapazität von MGÜ-Kabelstrecken bei Verwendung von extrudierten AC-Mittelspannungskabeln“, VDE-Hochspannungstechnik, online, 2020, pp. 371 – 376.
- [7] P. Ratheiser, U. Schichler, “DC Leakage Current Measurements: Contribution for the Qualification of extruded MVAC Cables for DC Operation”, ICPADM, online, 2021, pp. 450 – 453.
- [8] J. Yu et al., “Initial Design for ANGLE-DC Project: Challenges converting existing AC Cable and Overhead Line to DC Operation”, CIREN, Glasgow, Great Britain, 2017, Report 0974.
- [9] CIGRE WG B1.62, “Recommendations for testing DC extruded Cable Systems for Power Transmission at a rated Voltage up to and including 800 kV”, CIGRE TB 852, 2021.
- [10] D. Häring, F. Jenau, “DC Conductivity Measurements of Polymeric HVDC Insulation Materials under Consideration of a Dynamic Temperature Profile”, Jicable’19, Versailles, France, 2019, Report F2-6.
- [11] G. Mazzanti, M. Marzinotto, *Extruded Cables for High-Voltage Direct-Current Transmission – Advances in Research and Development*, Wiley-IEEE Press, New Jersey, USA, 2013.
- [12] G. Chen et al., “Review of High Voltage Direct Current Cables”, CSEE Journal of Power and Energy Systems, Vol. 1, Issue 2, 2015, pp. 9 – 21.
- [13] C. Freye, „Methoden und Aspekte zur Leitfähigkeitsanalyse von Isolationsmaterialien der Kabeltechnologie und zur Isolationskoordination für Systeme der Hochspannungsgleichstromübertragung (HGÜ)“, Dissertation, Technical University Dortmund, Germany, 2020.
- [14] IEC 62631-3-2, *Dielectric and resistive Properties of solid Insulating Materials - Part 3-2: Determination of resistive Properties (DC Methods) - Surface Resistance and Surface Resistivity*, 2015.